

Structure and Physical Properties of Low-Dimensional Molecular Conductors, [PXX][Fe^{III}(Pc)$(CN)_2$] and [PXX][Co^{III}(Pc)$(CN)_2$] (PXX = *peri*-xanthenoxanthene, Pc = phthalocyaninato)

Masaki Matsuda,* Takehiro Asari,† Toshio Naito,† Tamotsu Inabe,† Noriaki Hanasaki, and Hiroyuki Tajima

Institute for Solid State Physics, University of Tokyo, Kashiwanoha, Kashiwa, Chiba 277-8581

†Division of Chemistry, Graduate School of Science, Hokkaido University, Sapporo 060-0810

Received May 7, 2003; E-mail: masaki@issp.u-tokyo.ac.jp

A novel low-dimensional molecular conductor, [PXX][Fe^{III}(Pc)$(CN)_2$], has been synthesized. This salt contains the magnetic Fe^{III} ion ($S = 1/2$), and is isomorphous with [PXX][Co^{III}(Pc)$(CN)_2$] which includes the non-magnetic Co^{III} ion. In both salts, the [M^{III}(Pc)$(CN)_2$] (M = Fe or Co) units form a two-leg ladder chain. The two salts exhibit a similar temperature dependence of the thermoelectric power and a similar reflectance spectrum. The Fe^{III} salt shows semiconducting behavior in its electrical resistivity over the temperature range measured, while the isomorphous Co^{III} salt exhibits metallic behavior in its resistivity above 100 K. The difference in the transport properties between the two salts suggests that the conduction electrons in the Fe^{III} salt are seriously scattered by the local magnetic moment. Spontaneous magnetization is observed below 8 K in the Fe^{III} salt. Upon applying a magnetic field, the resistivity of the Fe^{III} salt drastically decreases below 50 K. The decrease in the resistivity is highly anisotropic to the field orientation. The field orientation dependence is highly consistent with the *g*-tensor anisotropy in the [Fe^{III}(Pc)$(CN)_2$] unit, suggesting that the negative magnetoresistance originates from the large π–d interaction self-contained in the [Fe^{III}(Pc)$(CN)_2$] unit.

Molecular conductors based on [Fe^{III}(Pc)$(CN)_2$] are good candidates for novel π–d systems.[1–3] The molecular arrangements of [M^{III}(Pc)$(CN)_2$] (M^{III} = Fe^{III} or Co^{III}) in a crystal adopt a slipped stack structure,[4] so that the intermolecular interaction significantly changes from that in the face-to-face-type [M(Pc)$_y$]X conductors (M = Ni, Co, Cu, etc.; X = I, AsF_6, etc.)[5–9] where direct metal–metal interaction exists.

Recently, the giant negative magnetoresistance has been found in TPP[Fe^{III}(Pc)$(CN)_2$]$_2$ (TPP = tetraphenylphosphonium).[3] This phenomenon is considered to be associated with the π–d interaction, that is the interaction between the π-conduction electrons and the local magnetic moments derived from the d_{yz} and d_{zx} orbitals of Fe^{III}. In molecular conductors based on [Fe^{III}(Pc)$(CN)_2$], the local magnetic moments should be embedded in the conduction path. Thus, it is promising that we can construct the π–d system, regardless of its crystal structure. In this context, we have tried to synthesize various molecular conductors containing [Fe^{III}(Pc)$(CN)_2$], and succeeded in obtaining PTMA$_x$[Fe^{III}(Pc)$(CN)_2$]·y(CH_3CN) (PTMA = phenyltrimethylammonium),[2] and [PXX][Fe^{III}(Pc)$(CN)_2$] (PXX = *peri*-xanthenoxanthene, the structure is shown in Scheme 1).

In this paper, we report the preparation, crystal structure, electrical resistivity, thermoelectric power, reflectance spectra, magnetic susceptibility, and magnetoresistance for the newly synthesized molecular conductor, [PXX][Fe^{III}(Pc)$(CN)_2$]. We compare the physical properties of this salt with those of [PXX][Co^{III}(Pc)$(CN)_2$], which is isomorphous with [PXX][Fe^{III}(Pc)$(CN)_2$]. In these salts, the [M^{III}(Pc)$(CN)_2$] units form a two-leg ladder chain along the *c*-axis. Because the ligand field is strong, the octahedral configuration imposes a low-spin state on the central metal ion, in this case Fe^{III} has an $S = 1/2$ magnetic moment while Co^{III} becomes non-magnetic. We show that [PXX][Fe^{III}(Pc)$(CN)_2$] exhibits the giant negative magnetoresistance in a similar manner as TPP[Fe^{III}(Pc)$(CN)_2$]$_2$.

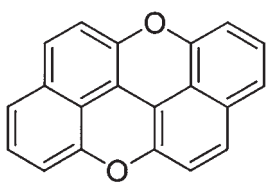

PXX

Scheme 1.

Experimental

Materials. The cation exchange was done by the metathesis of K_2[Fe^{II}(Pc)$(CN)_2$][1] with tetraheptylammonium iodide in acetonitrile. [(n-$C_7H_{15})_4N]_2$[Fe^{II}(Pc)$(CN)_2$] obtained was then oxidized to [(n-$C_7H_{15})_4N$][Fe^{III}(Pc)$(CN)_2$] by a stoichiometric amount of bromine in acetone. When bromine was added, the green solution immediately turned dark blue. After 8 h, purple blocks of [(n-$C_7H_{15})_4N$][Fe^{III}(Pc)$(CN)_2$] crystals were filtered off. The synthesis of PXX is described elsewhere.[10]

An electrocrystallization cell equipped with a glass frit between

Published on the web October 15, 2003; DOI 10.1246/bcsj.76.1935

two compartments was used for the electrolysis of the solution of $[(n\text{-}C_7H_{15})_4N][Fe^{III}(Pc)(CN)_2]$ (0.5–0.6 mmol dm^{-3}) and PXX (0.5–0.6 mmol dm^{-3}) in acetonitrile (ca. 35 mL). A constant current of typically 1.5 μA was applied between two platinum electrodes immersed in the solution of each compartment for 2–3 weeks at 20 °C. Black needle-shape and plate-shape crystals grew on the anode surface during the current flow, and were harvested by filtration. The needle-shape crystals were $[PXX][Fe^{III}(Pc)(CN)_2]$, and the plate-shape ones were considered to be $[PXX]_2[Fe^{III}(Pc)(CN)_2]\cdot CH_3CN$, as reported in the Co^{III} analog.[11]

The crystals of $[PXX][Co^{III}(Pc)(CN)_2]$ were prepared in a similar way reported elsewhere.[11]

X-ray Structure Analysis. Data collection for $[PXX][Fe^{III}(Pc)(CN)_2]$ was performed on an automated Rigaku AFC-7R diffractometer with graphite-monochromated Mo-Kα radiation using a standard method (2θ–ω scan, up to 55° in 2θ). Three standard reflections, which were monitored every 150 data measurements, showed no significant deviation in intensities. The crystal data is summarized in Table 1. The structure was solved by a direct method (SIR-92[12]), and the hydrogen atoms were placed at the calculated ideal positions. A full-matrix least-squares technique with anisotropic thermal parameters for non-hydrogen atoms and isotropic ones for hydrogen atoms, whose thermal parameters are 1.2 times that of the attached carbons, was employed for structure refinement using the teXsan program package.[13]

Crystallographic data has been deposited at the CCDC, 12 Union Road, Cambridge CB2 1EZ, UK and copies can be obtained on request, free of charge, by quoting the publication citation and the deposition number CCDC-201150.

Measurements. Electrical resistivity was measured with the current along the *c*-axis. The four electrical leads, gold wires of 20 μm in diameter, were attached to the crystal face using gold paste. In the low-resistive state ($R < 10^5$ Ω), the standard four-probe method was applied. In the high-resistive state, the measurement was switched to a two-probe method. The two-probe measurement was also extended into the higher temperature region, where the four-probe measurement gave reliable values, in order to make sure that the contact resistance was small enough and that its temperature dependence was negligible compared with that of the specimen. The switching temperature was 35–40 K for $[PXX][Fe^{III}(Pc)(CN)_2]$. The resistivity of $[PXX][Co^{III}(Pc)(CN)_2]$ was measured by the four-probe method at all temperatures. The reproducibility was also examined using several crystals. Thermoelectric power measurements were carried out using a system similar to that reported by Chaikin and Kwak.[14]

The polarized reflectance spectra of the single crystals of $[PXX][Fe^{III}(Pc)(CN)_2]$ and $[PXX][Co^{III}(Pc)(CN)_2]$ were measured by the use of an Olympus MMSP microspectrophotometer from 4200 cm^{-1} to 25000 cm^{-1}, and an FT-IR microspectrophotometer (Jasco FTIR 8900 μ) from 500 cm^{-1} to 4200 cm^{-1}. The crystal faces and the crystal axes of the sample were determined by the use of the X-ray diffraction technique.

Static magnetic susceptibility for the Fe^{III} salt was measured using Quantum Design MPMS (5S and R2) SQUID magnetometers. The applied field was 1 T. The core diamagnetic components were estimated to be -1.54×10^{-4} emu mol^{-1} and -1.38×10^{-4} emu mol^{-1} for PXX and $[Fe^{III}(Pc)(CN)_2]^-$, respectively. These values are given by the direct measurement of the susceptibility for neutral PXX, or by applying Pascal's law to the observed susceptibility data of $(TPP)_2[Fe^{II}(Pc)(CN)_2]$ and TPP·Br.

The resistivity under a high magnetic field was measured by the DC four-probe method over the entire temperature range (15–300 K) using a solenoid superconducting magnet (OXFORD Inst.). The sample was rotated inside the solenoid using a home-made sample holder.

Extended Hückel Calculation. The overlap integrals of HOMO's which form the conduction band in $[PXX][Fe^{III}(Pc)(CN)_2]$ were calculated on the basis of the extended Hückel approximation.[15] Because of the MO symmetry, the HOMO of the $[Fe^{III}(Pc)(CN)_2]$ unit consists of the π-orbital of the Pc ring, and does not contain the AO components for either the CN ligands or the Fe atom. Thus, we assumed that the HOMO of the $[Fe^{III}(Pc)(CN)_2]$ unit is equivalent to that of H_2Pc. The exponent and the ionization potential (Ryd) are as follows; C 2s, 1.625, −1.573; C 2p, 1.625, −0.838; N 2s, 1.950, −1.911; N 2p, 1.950, −0.985; H 1s, 1.0, −1.0.

Table 1. Data-Collection Conditions and Crystal Data of $[PXX][Fe^{III}(Pc)(CN)_2]$

Chemical formula	$C_{54}H_{26}N_{10}O_2Fe_1$
Formula weight	902.71
Crystal system	Monoclinic
Space Group	$P2_1/a$
a/Å	17.825(3)
b/Å	29.397(4)
c/Å	7.680(4)
β/°	102.29(3)
V/Å^3	3932(2)
Z	4
μ(Mo-Kα)/cm^{-1}	4.46
Temperature of data collection/K	293
No. of reflections measured	9668
No. of independent reflections observed	3979 [$I > 3\sigma(I)$]
R_{int}	0.045
R	0.044
R_w	0.043

$R = \sum ||F_0| - |F_c|| / \sum |F_0|$, $R_w = [\sum w(|F_0| - |F_c|)^2 / \sum wF_0^2]^{1/2}$.

Results and Discussion

Crystal Structure. Figure 1 shows the crystal structure of $[PXX][Fe^{III}(Pc)(CN)_2]$ at 293 K. This salt is isomorphous with $[PXX][Co^{III}(Pc)(CN)_2]$. The crystal structure of the Co^{III} salt is reported elsewhere.[11] In the crystal, the translationally related $[Fe^{III}(Pc)(CN)_2]$ units form a one-dimensional regular chain along the *c*-axis with an additional overlap with the neighboring chain, so that the $[Fe^{III}(Pc)(CN)_2]$ units form a two-leg ladder chain (Fig. 1(b)). The interplanar distances between peripheral benzene rings, with which the $[Fe^{III}(Pc)(CN)_2]$ units are stacked, are $d_{//} = 3.45$ Å and $d_{\perp} = 3.42$ Å. Here, $d_{//}$ and $d_{\perp}$ respectively denote the distance between the adjacent $[Fe^{III}(Pc)(CN)_2]$ units in the same chain and that between the adjacent units on the different chains forming the ladder. The corresponding values for the Co^{III} salt are $d_{//} = 3.46$ Å and $d_{\perp} = 3.40$ Å.[11]

To evaluate the effectiveness of the overlapping, we performed an extended Hückel calculation based on these structural data.[15] The overlap integrals between the Pc rings are estimated to be 6.6×10^{-3} along the intrachain direction ($s_{//}$) and 2.7×10^{-3} along the interchain direction ($s_{\perp}$). These val-

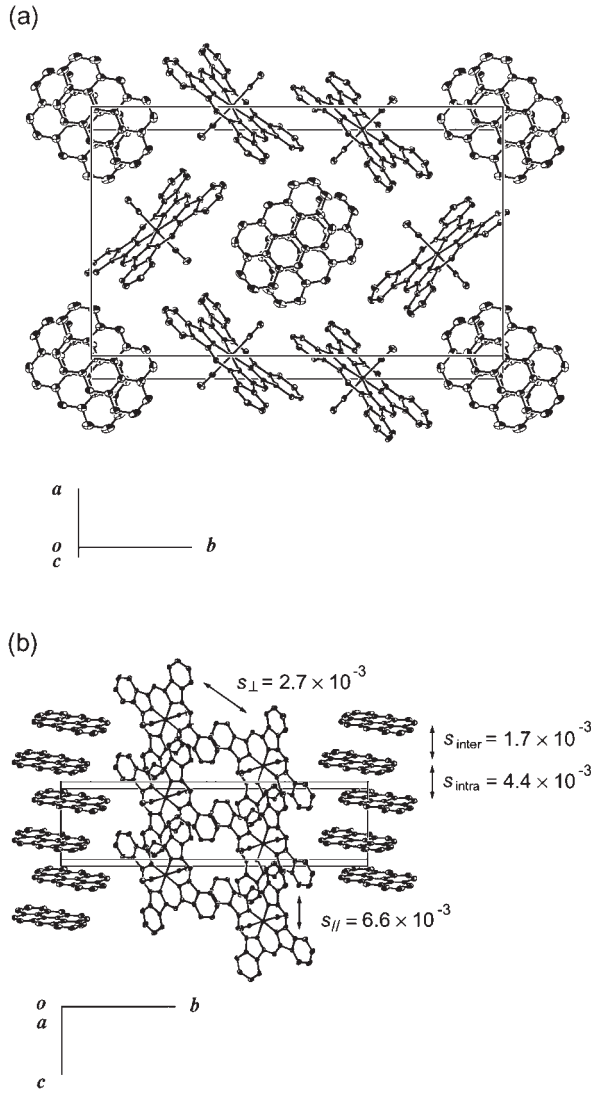

Fig. 1. Crystal structure of [PXX][Fe^{III}(Pc)$(CN)_2$]; (a) view normal to the *ab* plane and (b) the molecular arrangement in the *bc* plane.

ues are almost the same as the corresponding values in the Co^{III} salt, $s_{//} = 6.7 \times 10^{-3}$ and $s_\perp = 2.8 \times 10^{-3}$.[11]

The crystals of [PXX][M^{III}(Pc)$(CN)_2$] (M = Fe, Co) contain the PXX molecule and the [M^{III}(Pc)$(CN)_2$] unit with a stoichiometry of 1:1. The PXX molecules are dimerized and form a one-dimensional chain along the *c*-axis. The intradimer and interdimer overlap integrals (s_{intra}, s_{inter}) are 4.4×10^{-3} and 1.7×10^{-3}, respectively for both the Fe^{III} salt and the Co^{III} salt. The effective charge δ in $[PXX]^{\delta+}[Co^{III}(Pc)(CN)_2]^{\delta-}$ has been reported to be close to 0.5.[11] Since the Fe^{III} salt is isostructural with the Co^{III} salt, and the bond lengths of both the Pc ring and PXX molecule in the Fe^{III} salt are almost the same to those in the Co^{III} salt, it is reasonable to assume that the effective charge in $[PXX]^{\delta+}[Fe^{III}(Pc)(CN)_2]^{\delta-}$ is also close to 0.5. As we discuss later, the similarity of the infrared reflectance spectra in both salts confirms this assumption.

Though both the PXX and [M^{III}(Pc)$(CN)_2$] units are partially oxidized, the charge transport is expected to be sustained primarily in the regular Pc ladder chain rather than the dimerized PXX chain.

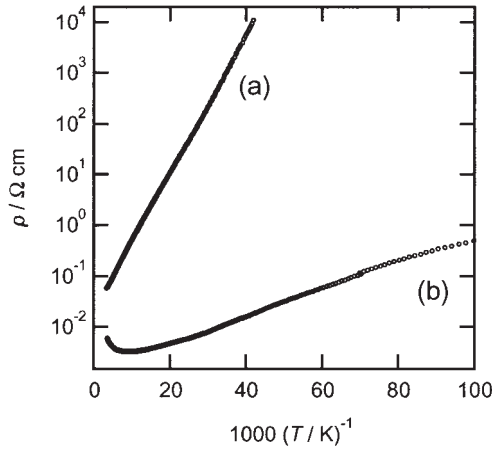

Fig. 2. Temperature dependence of the resistivity along the *c*-axis (ρ) for (a) [PXX][Fe^{III}(Pc)$(CN)_2$] and (b) [PXX]-[Co^{III}(Pc)$(CN)_2$].

Electrical Resistivity and Thermoelectric Power. Figure 2 shows the temperature dependence of the resistivity along the *c*-axis for [PXX][Fe^{III}(Pc)$(CN)_2$] and [PXX]-[Co^{III}(Pc)$(CN)_2$]. The resistivity of the Fe^{III} salt at room temperature is 3.3×10^{-2} Ω cm, which is nearly one order of magnitude higher than that of the Co^{III} salt (6.0×10^{-3} Ω cm).[11] The Fe^{III} salt shows semiconducting behavior, and the activation energy (E_a) for conduction varies slightly around 50 K ($E_a = 0.022$ eV around 65 K and $E_a = 0.027$ eV around 30 K). On the other hand, the Co^{III} salt shows metallic behavior above 100 K, and very weak semiconducting behavior below 100 K. Considering the semiconducting behavior of other Co^{III} salts having a one-dimensional strucuture,[2,16] the metallic behavior above 100 K for the Co^{III} salt may be due to the ladder structure.[4,11] The resistivity ratio of the Fe^{III} salt to the Co^{III} salt is approximately 10^5 at 25 K.

Figure 3 shows the temperature dependence of the thermoelectric power (*S*) for [PXX][Fe^{III}(Pc)$(CN)_2$] and [PXX]-[Co^{III}(Pc)$(CN)_2$]. The thermoelectric power around room temperature is positive in both salts. This is consistent with the fact that holes are generated by the oxidation of the closed-shell Pc^{2-} in $[M^{III}(Pc)(CN)_2]^-$. When the effective charge of the [M^{III}(Pc)$(CN)_2$] unit is −0.5, the formal charge of the Pc

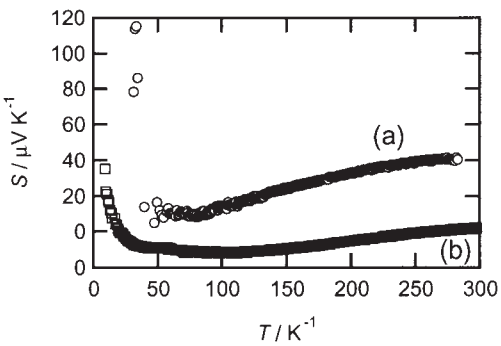

Fig. 3. Temperature dependence of the thermoelectric power along the *c*-axis (*S*) for (a) [PXX][Fe^{III}(Pc)$(CN)_2$] and (b) [PXX][Co^{III}(Pc)$(CN)_2$]. Note the scale offset of 20 μV K^{-1} for (a).

ring is −1.5, resulting in a 3/4-filled π-conduction band. On lowering the temperature, the thermoelectric power gradually decreases down to ca. 100 K, and then gradually increases. This behavior is common for both salts. According to the standard model based on the Boltzmann equation, the thermoelectric power of the metal is given by $S \propto T$, while that of the semiconductor is given by $S \propto T^{-1}$. In this respect, the temperature dependence of the thermoelectric power for the Co^{III} salt is consistent with the behavior of the electrical resistivity above 100 K. What is puzzling to us is the thermoelectric power data of the Fe^{III} salt. The data seems to suggest that there is a metal-insulator transition around 50 K in this salt, while the resistivity data exhibit semiconducting behavior over the entire temperature range measured. Similar puzzles are encountered in TPP[M^{III}(Pc)(CN)$_2$]$_2$ and (PTMA)$_x$[M^{III}(Pc)(CN)$_2$]·y(CH$_3$CN).[1,2,16] According to Mott, the thermoelectric power of a semiconductor whose Fermi energy is below the mobility edge exhibits $S \propto T$ behavior, while the electrical resistivity exhibits semiconducting behavior.[17] If we accept this scenario, there should be a mobility edge in [PXX]-[Fe^{III}(Pc)(CN)]. The mobility edge arises from the random potential in a crystal. What is the origin of the random potential in this salt? One may consider the random potential to be associated with the structural disorder. However, we ruled out this possibility, since serious disorder was not found in the X-ray diffraction measurement. At the present stage, we are considering the fluctuation of the local magnetic moments at the Fe^{III} site as the source of the random potential in the π-conduction electrons in the Pc ring. In this case, the semiconducting behavior of the resistivity in the Fe^{III} salt is attributable to the scattering of the conduction electrons by the local magnetic moments, rather than to the energy gap formation.

Optical Properties. Figure 4 shows the reflectance spectra of [PXX][Fe^{III}(Pc)(CN)$_2$] and [PXX][Co^{III}(Pc)(CN)$_2$] at room temperature for the polarizations parallel to the c-axis (E // c) and to the b-axis (E // b). The similarity of the spectral shapes in both salts strongly suggests that the [M^{III}(Pc)(CN)$_2$] units are in the same oxidation state in the salts, as already discussed in the X-ray study. The dispersion around 9000 cm^{-1} can be assigned to the charge-transfer excitation between different kinds of molecular orbitals.[1] We expected additional optical transitions associated with the ladder formation in the E // b spectrum. However, no significant difference between the E // a^* spectrum (not shown in the Fig. 4) and the E // b spectrum was observed. This suggests that chain–chain interactions in the ladder are not strong.

The reflectance spectra parallel to the c-axis were analyzed using the Lorentz-type complex dielectric function given by:

$$R(\omega) = \left| \frac{\sqrt{\varepsilon(\omega)} - 1}{\sqrt{\varepsilon(\omega)} + 1} \right|^2, \quad (1)$$

and the relation between the reflectance and the complex dielectric function:

$$\varepsilon(\omega) = \varepsilon_\infty - \frac{\omega_p^2}{\omega^2 - \omega_0^2 - i\gamma\omega} - \sum_m \frac{\Omega_{pm}^2}{\omega^2 - \Omega_m^2 - i\Gamma_m\omega}. \quad (2)$$

Here, ω_0 and ω_p correspond to the gap energy and plasma frequency determined for the lowest inter-band transition, and

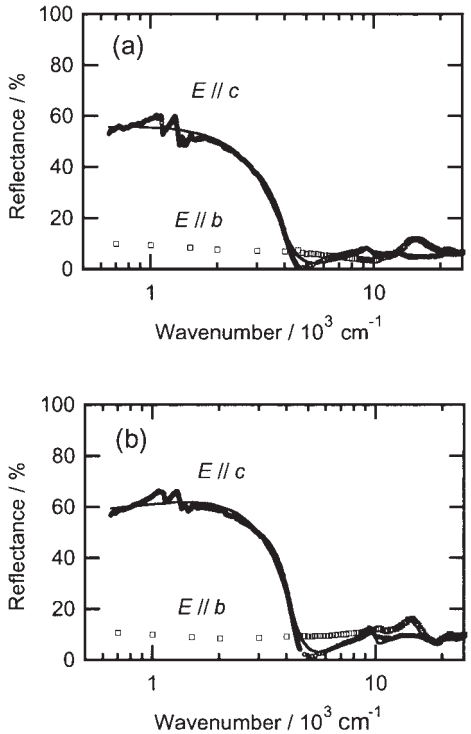

Fig. 4. Polarized optical reflectance spectra of (a) [PXX][Fe^{III}(Pc)(CN)$_2$] and (b) [PXX][Co^{III}(Pc)(CN)$_2$]. The solid lines are the best fits obtained by the parameter set listed in Table 2.

Table 2. Optical and Electrical Parameters Obtained from the Reflectance Spectra

	[PXX][Fe^{III}(Pc)(CN)$_2$]	[PXX][Co^{III}(Pc)(CN)$_2$]
ε_∞	2.84	3.57
ω_0/cm^{-1}	1104	1226
ω_p/cm^{-1}	7270	8680
γ/cm^{-1}	1918	1643
Ω_1/cm^{-1}	9689	9868
Ω_{p1}/cm^{-1}	3049	3201
Γ_1/cm^{-1}	1079	911
Ω_2/cm^{-1}	13419	15949
Ω_{p2}/cm^{-1}	4949	7084
Γ_2/cm^{-1}	2899	3723
d/Å	7.680	7.678
V_c/Å^3	983	976
t/eV	0.083	0.117

Ω_m and Ω_{pm} is the excitation energy and the plasma frequency of the charge-transfer band and intra-molecular excitation, respectively. The best fits to the model are shown by solid lines in Fig. 4. The parameters, ω_0 and ω_p, which give the best fits are listed in Table 2. The gap energy (= ω_0), about 1000 cm^{-1}, is inconsistent with the metallic behavior for the Co^{III} salt and about twice the gap energy deduced from the electrical resistivity for the Fe^{III} salt ($2E_a$ = 0.06 eV = 480 cm^{-1} = 700 K). The appearance of the optical gap in the one-dimensional metallic salt is a well-known phenomenon. This phenomenon is attributable to the strong electron–electron correlation effects.[18–20] Assuming the sys-

tem to be one-dimensional, we apply the tight-binding model to the spectrum analysis. In this model, the transfer integral, t, is given by[21]

$$t = \frac{\hbar^2 V_c \omega_p^2}{16e^2 d^2 \sin(\pi\nu/2)}, \quad (3)$$

where V_c is the volume fraction of the $M^{III}(Pc)(CN)_2$ unit, ω_p is plasma frequency, d is the spacing between the $[M^{III}(Pc)(CN)_2]$ units along the stacking axis and ν is the electron density in the HOMO of the $[M^{III}(Pc)(CN)_2]$ unit. Using Eq. 3 and $\nu = 1.5$, we estimated the transfer integrals listed in Table 2. The values of the transfer integrals in $[PXX][M^{III}(Pc)(CN)_2]$ (M = Fe and Co) are smaller than those of the TPP and PTMA salts.[1,2,16] The smaller transfer integrals of the PXX salts are consistent with the smaller overlap integrals given by the extended Hückel calculation.

Magnetic Susceptibility. Figure 5 shows the temperature dependence of the magnetic susceptibility for the randomly orientated samples of $[PXX][Fe^{III}(Pc)(CN)_2]$. Since the average charge density is approximately 0.5 for the PXX molecule, it may be plausible to assume that PXX molecules form a dimer unit accommodating one unpaired electron. Thus there are two kinds of local moments in the Fe^{III} salt; one comes from a π-radical spin localized on a PXX dimer, and the other from the Fe^{III} ion in the low-spin state ($S = 1/2$). If we assume $S = 1/2$ and $g = 2.0$ for these moments, the $\chi_p T$ value at 300 K is expected to be around 0.5625 emu mol^{-1} K. However, the observed $\chi_p T$ value at 300 K (0.881 emu mol^{-1} K) is much larger than this value. According to the ESR experiments, the g-factors of the $[Fe^{III}(Pc)(CN)_2]$ unit are $g_1 = 3.6$, $g_2 = 1.1$ and $g_3 = 0.5$.[22] Here, g_1 denotes the g-factor for the static magnetic field approximately perpendicular to the Pc ring, and g_2 and g_3 denote the two g-factors for the field approximately parallel to the Pc ring. When the crystals are completely randomly-orientated, the value of $\chi_p T$ at 300 K is estimated to be 0.637 emu mol^{-1} K using $g_{av}(\equiv \sqrt{(g_1^2 + g_2^2 + g_3^2)/3}) = 2.19$. The observed value is still larger than this estimated value. One possible answer to this disagreement is to consider the partial orientation of the crystals under the magnetic fields. The torque caused by the magnetic field tends to orient the crystal, so that the crystal axis having the highest susceptibility component coincides with the field direction. Consequently, the observed susceptibility should be larger than that of random-orientated crystals.

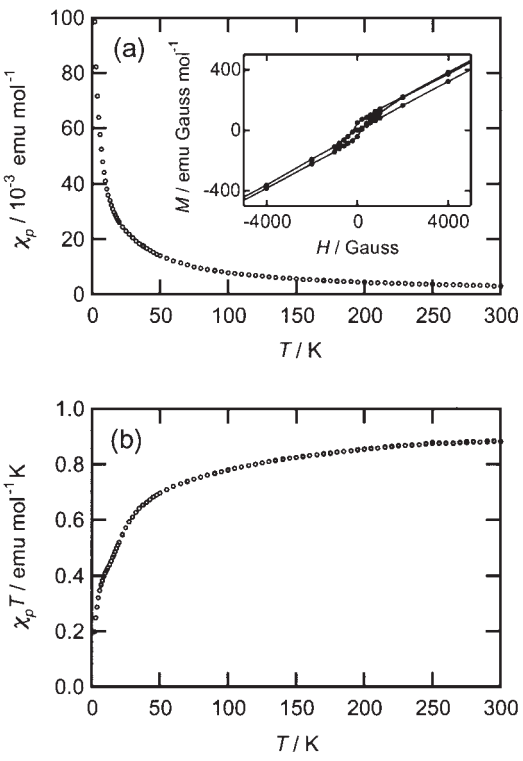

Fig. 5. Temperature dependence of the magnetic susceptibility (χ_p) for randomly-orientated polycrystalline samples of $[PXX][Fe^{III}(Pc)(CN)_2]$. (a) χ_p vs T and (b) $\chi_p T$ vs T plot. Inset in the upper figure is a magnetization curve of $[PXX][Fe^{III}(Pc)(CN)_2]$ at 2 K.

At temperatures below 50 K, $\chi_p T$ of the Fe^{III} salt remarkably decreases with a lowering of the temperature. The decrease is due to the antiferromagnetic interaction between the $[Fe^{III}(Pc)(CN)_2]$ units. Since the shortest distance between Fe^{III} atoms is more than 7.5 Å, the antiferromagnetic interaction should be mediated by π-electrons in the Pc rings.

Below 8 K, $[PXX][Fe^{III}(Pc)(CN)_2]$ exhibits residual magnetization which manifests the weak ferromagnetism. The magnetization curve at 2 K is shown in the inset of Fig. 5. The amount of residual magnetization is 8.3×10^{-3} μ_B at 2 K. A similar weak ferromagnetism is observed in TPP-$[Fe^{III}(Pc)(CN)_2]_2$ and in $(PTMA)_x[Fe^{III}(Pc)(CN)_2]\cdot y(CH_3CN)$.

Magnetoresistance. Figure 6 shows the temperature dependence of the magnetoresistance under a magnetic field of 16 T for $[PXX][Fe^{III}(Pc)(CN)_2]$. We applied a magnetic field parallel to the c-axis (B // c) and perpendicular to the c-axis (B // a^* and B // b). A negative magnetoresistance is observed below 50 K for all directions, but has a large anisotropy with the field direction. The resistivity ratio at 20 K is $\rho(B = 16\ T\ //\ a^*)/\rho(0) = 0.25$, $\rho(B = 16\ T\ //\ b)/\rho(0) = 0.26$ and $\rho(B = 16\ T\ //\ c)/\rho(0) = 0.55$.

Recently, we have proposed that the magnetic-field-orientation dependence of the negative magnetoresistance for TPP$[Fe^{III}(Pc)(CN)_2]_2$ is associated with the molecular orientation of the $[Fe^{III}(Pc)(CN)_2]$ unit.[23] In this model, the negative magnetoresistance is largest for the field orientation perpendicular to the Pc plane, and monotonously decreases with increasing tilt of the field. By applying this model to $[PXX][Fe^{III}(Pc)(CN)_2]$, it is expected that the B // a^* magnetoresistance would be comparable to the B // b magnetoresistance and much larger than the B // c magnetoresistance. This is consistent with the observation in Fig. 6.

The enhancement of semiconducting behavior and the negative magnetoresistance appear below 50 K. Below this temperature, the thermoelectric power abruptly increases. Considering this behavior, there may be additional scattering of the itinerant electron in $[PXX][Fe^{III}(Pc)(CN)_2]$ below 50 K. A further study is necessary to clarify the origin of the scattering and giant negative magnetoresistance.

In conclusion, we have succeeded in synthesizing a two-leg ladder molecular conductor having the magnetic Fe^{III} ion. The obtained salt, $[PXX][Fe^{III}(Pc)(CN)_2]$, is isomorphous with

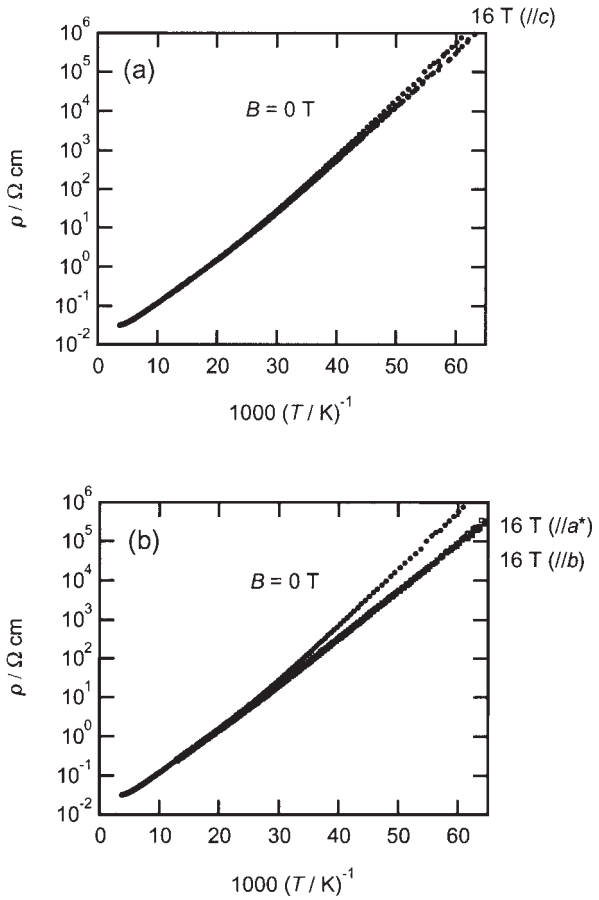

Fig. 6. Temperature dependence of the magnetoresistance for [PXX][Fe^{III}(Pc)(CN)$_2$]. (a) The static magnetic field (16 T) is applied parallel to the *c*-axis (b) The static magnetic field (16 T) is applied parallel to the a^*-axis (open square) or to the *b*-axis (closed square).

[PXX][Co^{III}(Pc)(CN)$_2$], which includes non-magnetic Co^{III} instead of magnetic Fe^{III}. The reflectance spectra of the Fe^{III} salt are similar to those of the Co^{III} salt. The transfer integrals estimated from the reflectance spectra are approximately 0.1 eV along the one-dimensional chain for both salts. In spite of the small transfer integral along the one-dimensional chain, the Co^{III} salt shows clear metallic behavior. Contrary to the Co^{III} salt, the Fe^{III} salt exhibits semiconducting behavior. The difference of the electrical behavior between the Fe^{III} and the Co^{III} salts suggests that the conduction electron in the Fe^{III} salt is seriously scattered by the local magnetic moment in Fe^{III}. The resistance measurements under a high magnetic field revealed the giant negative magnetoresistance for the Fe^{III} salt. The observed large anisotropy in the negative magnetoresistance can be accurately explained by taking into account the anisotropic *g*-tensor in the [Fe^{III}(Pc)(CN)$_2$] unit. This result suggests that the giant negative magnetoresistance originates from the large π–d interaction self-contained in the [Fe^{III}(Pc)(CN)$_2$] unit.

Part of this work was performed using facilities in the Spectroscopy Laboratory, the Material Design and Characterization Laboratory, ISSP. This work was partly supported by the Grant-in-Aid for Scientific Research, from the Ministry of Education, Culture, Sports, Science and Technology.

References

1 M. Matsuda, T. Naito, T. Inabe, N. Hanasaki, H. Tajima, T. Otsuka, K. Awaga, B. Narymbetov, and H. Kobayashi, *J. Mater. Chem.*, **10**, 631 (2000).

2 M. Matsuda, T. Naito, T. Inabe, N. Hanasaki, and H. Tajima, *J. Mater. Chem.*, **11**, 2493 (2001).

3 N. Hanasaki, H. Tajima, M. Matsuda, T. Naito, and T. Inabe, *Phys. Rev. B: Condens. Matter*, **62**, 5839 (2000).

4 T. Inabe, *J. Porphyrins Phthalocyanines*, **5**, 3 (2001).

5 J. Martinsen, J. L. Stanton, R. L. Greene, J. Tanaka, B. M. Hoffman, and J. A. Ibers, *J. Am. Chem. Soc.*, **107**, 6915 (1985).

6 M. Y. Ogawa, B. M. Hoffman, S. Lee, M. Yudkowsky, and W. P. Halperin, *Phys. Rev. Lett.*, **57**, 1177 (1986); M. Y. Ogawa, J. Martinsen, S. M. Palmer, J. L. Stanton, J. Tanaka, R. L. Greene, B. M. Hoffman, and J. A. Ibers, *J. Am. Chem. Soc.*, **109**, 1115 (1987).

7 M. Y. Ogawa, S. M. Palmer, K. Liou, G. Quirion, J. A. Thompson, M. Poirier, and B. M. Hoffman, *Phys. Rev. B: Condens. Matter*, **39**, 10682 (1989); G. Quirion, M. Poirier, K. K. Liou, and B. M. Hoffman, *Phys. Rev. B: Condens. Matter*, **43**, 860 (1991).

8 T. Hiejima and K. Yakushi, *J. Chem. Phys.*, **103**, 3950 (1995); H. Yamakado, T. Ida, A. Ugawa, K. Yakushi, K. Awaga, Y. Maruyama, K. Imaeda, and H. Inokuchi, *Synth. Met.*, **62**, 169 (1994).

9 C. J. Schramm, R. P. Scaringe, D. R. Stojakovic, B. M. Hoffman, J. A. Ibers, and T. J. Marks, *J. Am. Chem. Soc.*, **102**, 6702 (1980).

10 T. Asari, N. Kobayashi, T. Naito, and T. Inabe, *Bull. Chem. Soc. Jpn.*, **74**, 53 (2001).

11 S. Takano, T. Naito, and T. Inabe, *Chem. Lett.*, **1998**, 1249.

12 A. Altomare, M. C. Burla, M. Camalli, M. Cascarano, C. Giacovazzo, A. Guagliardiand, and G. Polidori, *J. Appl. Crystallogr.*, **27**, 435 (1994).

13 "teXsan; Crystal Structure Analysis Package," Molecular Structure Corporation, 3200 Research Forest Drive, The Woodlands, TX 77381 (1985 and 1992).

14 P. M. Chaikin and J. F. Kwak, *Rev. Sci. Instrum.*, **46**, 218 (1975).

15 T. Mori, A. Kobayashi, Y. Sasaki, H. Kobayashi, G. Saito, and H. Inokuchi, *Bull. Chem. Soc. Jpn.*, **57**, 627 (1984).

16 H. Hasegawa, T. Naito, T. Inabe, T. Akutagawa, and T. Nakamura, *J. Mater. Chem.*, **8**, 1567 (1998).

17 N. Mott, "Conduction in Non-Crystalline Materials," Clarendon Press, Oxford (1987).

18 T. Giamarchi, *Physica B*, **230**, 975 (1997).

19 D. Jérome and H. J. Schulz, *Adv. Phys.*, **31**, 299 (1982).

20 T. Yamamoto, H. Tajima, J. Yamaura, S. Aonuma, and R. Kato, *J. Phys. Soc. Jpn.*, **68**, 1384 (1999); H. Tajima, *Solid State Commun.*, **113**, 279 (2000).

21 J. B. Torrance, B. A. Scott, B. Welber, F. B. Kaufman, and P. E. Seiden, *Phys. Rev. B: Condens. Matter*, **19**, 730 (1979).

22 N. Hanasaki, M. Matsuda, H. Tajima, T. Naito, and T. Inabe, *Synth. Met.*, **133–134**, 519 (2003).

23 H. Tajima, N. Hanasaki, M. Matsuda, T. Naito, and T. Inabe, *J. Solid State Chem.*, **168**, 509 (2002).